JOC Article

Quantitative Active Transport in [2]Rotaxane Using a One-Shot Acylation Reaction toward the Linear Molecular Motor

Yoshimasa Makita,*,† Nobuhiro Kihara,‡ and Toshikazu Takata*,§

Department of Chemistry, Osaka Dental University, 8-1 Kuzuhahanazono-cho, Hirakata, Osaka, 573-1121, Japan, Department of Chemistry, Faculty of Science, Kanagawa University, 2946 Tsuchiya, Hiratsuka 259-1293, Japan, and Department of Organic and Polymeric Materials, Tokyo Institute of Technology, Ookayama, Meguro-ku, Tokyo 152-8552 Japan

makita@cc.osaka-dent.ac.jp; ttakata@polymer.titech.ac.jp

Received July 4, 2008

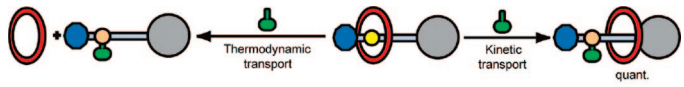

100% efficient ACTIVE TRANSPORT by the potential surface of axle

A rotaxane consisting of a crown ether wheel and a secondary ammonium salt axle, on which a neopentyl-type end-cap was placed close to the ammonium moiety, was prepared. When the rotaxane was treated by excess triethylamine, the wheel component thermodynamically moved over the proximate neopentyl group to deconstruct the interlocked structure. The wheel component in the rotaxane, however, quantitatively moved against the proximate end-cap by the action of trifluoroacetic anhydride in the presence of excess triethylamine. This motion, which was driven by the simple one-shot acylation reaction, can be referred as the active transport. When the distant end-cap is of the neopentyl-type, the axle can be thermally dethreaded from the distant end-cap after the acylative transport. The series of the wheel movement controlled by the neopentyl group can be the basic motion of the unidirectional linear molecular motor.

Introduction

Since molecular motors,[1] rotational motors such as ATPase,[2] and linear motors such as the actin−myosin system[3] and kinesin−microtube system[4] are essential components in living systems, the construction of artificial molecular motors has received considerable attention. Although various artificial rotational molecular motors[5] and stretching molecules[6] have been studied thus far, only limited research on artificial linear molecular motors are reported.[7]

In stretching molecular systems, the on−off mode is thermodynamically controlled: the mobile component migrates to the thermodynamically most favored position on the track, which can be changed by an external stimulus. It seems that an artificial linear molecular motor can be constructed as an extension of the stretching system.[8] However, linear molecular motor and stretching system are basically different because the track of the natural linear molecular motor has polymeric structure. Since the polymeric track in the linear molecular motor exhibits a periodic potential surface (Figure 1), the forward and backward sides of the motor are thermodynamically and kinetically

* To whom correspondence should be addressed. (Y.M.) Tel: +81-72-864-3162. Fax: +81-72-864-3162. (T.T.) Tel: +81-3-5734-2898. Fax: +81-3-5734-2888.
† Osaka Dental University.
‡ Kanagawa University.
§ Tokyo Institute of Technology.

(1) *Molecular Motors*; Schliwa, M., Ed.; Wiley-VCH: Weinheim, Germany, 2003.
(2) (a) Boyer, P. D. *Angew. Chem., Int. Ed.* **1998**, *37*, 2296–2307. (b) Walker, J. E. *Angew. Chem., Int. Ed.* **1998**, *37*, 2308–2319.
(3) (a) Finer, J. T.; Simmons, R. M.; Spudich, J. A. *Nature* **1994**, *368*, 113–119. (b) Rief, M.; Rock, R. S.; Mehta, A. D.; Mooskeker, M. S.; Cheney, R. E.; Spudich, J. A. *Proc. Natl. Acad. Sci. U.S.A.* **2000**, *97*, 9482–9486.
(4) (a) Vale, R. D.; Milligan, R. A. *Science* **2000**, *88*, 88–95. (b) Visscher, K.; Schnitzer, M. J.; Block, S. M. *Nature* **1999**, *400*, 184–189.
(5) (a) Kay, E. R.; Leigh, D. A.; Zerbetto, F. *Angew. Chem., Int. Ed.* **2007**, *46*, 72–191. (b) Koumura, N.; Zjilstra, R. W. J.; van Delden, R. A.; Harada, N.; Feringa, B. L. *Nature* **1999**, *401*, 152–155. (c) Vicario, J.; Walko, M.; Meetsma, A.; Feringa, B. L. *J. Am. Chem. Soc.* **2006**, *128*, 5127–5135. (d) Leigh, D. A.; Wong, J. K. Y.; Dehez, F.; Zerbetto, F. *Nature* **2003**, *424*, 174–179. (e) Hernández, J. V.; Kay, E. R.; Leigh, D. A. *Science* **2004**, *306*, 1532–1537. (f) Kelly, T. R.; De Silva, H.; Silva, R. A. *Nature* **1999**, *401*, 150–152. (g) Kelly, T. R.; Cai, X.; Damkaci, Fehmi, Sceeletha, B.; Panicker, B. T.; Bushell, S. M.; Cornella, I.; Piggott, M. J.; Salives, R.; Cavero, M.; Zhao, Y.; Jasmin, S *J. Am. Chem. Soc.* **2007**, *129*, 376–386. (h) Fletcher, S. P.; Dumur, F.; Pollard, M. M.; Feringa, B. L. *Science* **2005**, *301*, 80–82.
(6) (a) Badjiæ, J. D.; Balzani, V.; Credi, A.; Silvi, S.; Stoddart, J. F. *Science* **2004**, *303*, 1845–1849. (b) Liu, Y.; Flood, A. H.; Bonvallet, P. A.; Vignon, S. A.; Northrop, B.; Tseng, H.-R.; Jeppesen, J.; Huang, T. J.; Brough, B.; Baller, M.; Magonov, S.; Solares, S.; Goddard, W. A., III; Ho, C.-M.; Stoddart, J. F. *J. Am. Chem. Soc.* **2005**, *127*, 9745–9759. (c) Jiménez, M. C.; Dietrich-Buchecker, C. O.; Sauvage, J.-P. *Angew. Chem., Int. Ed.* **2000**, *39*, 3284–3287.
(7) (a) Chatterjee, M. N.; Kay, E. R.; Leigh, D. A. *J. Am. Chem. Soc.* **2006**, *128*, 4058–4073. (b) Serreli, V.; Lee, C.-F.; Kay, E. R.; Leigh, D. A. *Nature* **2007**, *445*, 523–527. (c) Alvarez-Pérez, M.; Goldup, S. M.; Leigh, D. A.; Slawin, A. M. Z. *J. Am. Chem. Soc.* **2008**, *130*, 1836–1838.

10.1021/jo8013726 CCC: $40.75 © 2008 American Chemical Society
Published on Web 10/28/2008

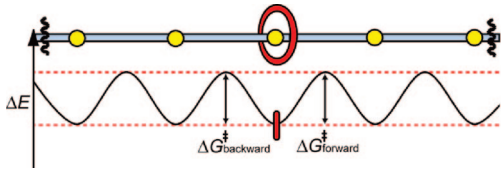

FIGURE 1. Schematic representation of a [2]rotaxane-based unidirectional linear molecular motor and its periodic potential surface. The track has a polymeric structure and exhibits periodic potential surface. Here, $\Delta G_{backward} = \Delta G_{forward} = 0$, and the values of $\Delta G^{\ddagger}$ for both forward and backward transpositions to the next station are identical.

indistinguishable. In other words, since every station on the track interacts with the moving component with the same stability, every station is thermodynamically identical ($\Delta G_{backward} = \Delta G_{forward} = 0$), and the activation energies ($\Delta G^{\ddagger}$) of the forward and backward movements are exactly same. It seems that unidirectional molecular motor can be realized if the moving component interacts with the track to decrease $\Delta G^{\ddagger}_{backward}$ or $\Delta G^{\ddagger}_{forward}$ exclusively. However, this mechanism is contrary to the second law of thermodynamics. Since unidirectional movement is an entropically undesired change ($\Delta S < 0$), the supply of free energy is necessary. If the moving component induced the exclusive change in $\Delta G^{\ddagger}$ by any interaction, unidirectional movement could take place without the additional supply of free energy.[9] Thus, the molecular motor must furnish an active transport system in which thermodynamically unfavored change is induced by a certain free energy source.

To achieve a unidirectional movement by the active transport, a thermodynamically metastable state should be prepared by the local gradient of the potential surface before it is kinetically fixed.[5f] Most of the artificial molecular motors succeeded in providing such a control on the basis of photoreactions.[5b−e] For example, Leigh reported a linear active transport system,[7b] where the wheel component of rotaxane was transferred toward a thermodynamically undesired direction by the photo $E-Z$ isomerization of olefine. Natural molecular motors, however, are driven by the action of ATP. Although active transport systems were realized with the chemical energy in the rotational system,[5f−h] only one example of a chemical-energy-based artificial linear active transport system has been reported very recently by Leigh.[7c] Leigh's system is based on the asymmetric acylation of a hydroxy group bearing [2]rotaxane. However, the efficiency of active transport in this system is low; hence, it seems difficult to construct a linear molecular motor that moves on a long track using multiple chemical reactions.

To construct the active transport system with high efficiency, we used [2]rotaxane system because wheel component and the axle component are inseparable in rotaxane. Using rotaxane, we can focus our effort to the construction of potential surface on the axle as the track. In this paper, we wish to report a 100% efficient active transport that is energized by a simple one-shot acylation reaction of [2]rotaxane by providing the appropriate potential surface on the axle component. The vision toward the linear molecular motor is also described based on this active transport system.

Results and Discussion

We have studied the acylative neutralization of rotaxane consisting of an ammonium salt axle and a crown ether wheel.[10] The wheel migrates to the less crowded side on the axle in the resulting rotaxane. Although the dethreading of the axle is the thermodynamically favored process without the attractive interaction between the wheel and the axle components, the bulky end-caps at the end of the axle prevent the dethreading. Based on this system, we designed an active transport system, as illustrated in Figure 2.

At first, rotaxane has an asymmetric axle, where the end-caps are small enough to allow the dethreading. The station (an ammonium salt moiety) is located close to one of the two end-caps, while there exists some space between the station and the other end-cap (Figure 2a). Therefore, the gradient of the potential surface around the station is also asymmetric; it is steep for the proximate end-cap and gradual for the distant end-cap.

Due to the strong interaction between the station and the wheel, $\Delta G^{\ddagger}$ for the dethreading is so large that dethreading is prevented. During the treatment of rotaxane with a tertiary amine, the wheel component starts migrating because the interaction between the crown ether and the ammonium moiety is lost (Figure 2b). Initially, the probability of the population of the wheel component will be maximum at the center of the axle because of the gradient of the potential surface; the tentative position is independent of both the global thermodynamic stability and the activation energy of the wheel dethreading. If the system is kept in this condition, the wheel will be escaped out over each end-cap with same probability.

When a bulky substituent is introduced on the amino group by the rapid acylation reaction, the distribution of the wheel on the axle component is fixed, and dethreading beyond the proximate end-cap is selectively forbidden (Figure 2c). If the acylation is slow, dethreading occurs at both the end-caps. For a successful active transport that allows one-way migration, the end-cap must be bulky enough to attenuate the thermal dethreading and produce a steep potential surface before the completion of acylation; however, it must be smaller than the cavity of the wheel to allow dethreading to take place after acylation.

To explore an appropriate end-cap group that allows active transport, a series of rotaxanes with asymmetric axles were synthesized and their acylation was examined (Scheme 1). The distant end-cap was fixed to the 3,5-dimethylphenyl group. Since this group is known to be so bulky that dethreading can be completely prevented for the dibenzo-24-crown-8 (DB24C8) wheel, the active transport can be detected easily.

(8) (a) Sauvage, J.-P.; Dietrich-Buchecker, C. *Molecular Catenanes, Rotaxanes, and Knots*; Wiley-VCH: Weinheim, Germany, 1999. (b) Sauvage, J.-P. *Molecular Machines and Motors; Structure and Bonding*; Springer: Berlin, Germany, 2001; Vol. 99. (c) Balzani, V.; Credi, A.; Venturi, M. *Concepts and Perspectives for the Nanoworld*, 2nd ed.; Wiley-VCH: Weinheim, Germany, 2008. (d) Balzani, V.; Credi, A.; Raymo, F. M.; Stoddart, J. F. *Angew. Chem., Int. Ed.* **2000**, *39*, 3349–3391.

(9) (a) Kelly, T. R.; Tellitu, I.; Sestelo, J. P. *Angew. Chem., Int. Ed. Engl.* **1997**, *36*, 1866–1868. (b) Kelly, T. R.; Sestelo, J. P.; Tellitu, I. *J. Org. Chem.* **1998**, *63*, 3655–3665.

(10) (a) Kawasaki, H.; Kihara, N.; Takata, T. *Chem. Lett.* **1999**, 1015–1016. (b) Kihara, N.; Tachibana, Y.; Kawasaki, H.; Takata, T. *Chem. Lett.* **2000**, 506–507. (c) Tachibana, Y.; Kawasaki, H.; Kihara, N.; Takata, T. *J. Org. Chem.* **2006**, *71*, 5093–5104. In the case of rotaxanes with two stations on the axle, it is known that the deprotonation of the ammonium moiety is fast; see: (d) Garaude, S.; Silvi, S.; Venturi, M.; Credi, A.; Flood, A. H.; Stoddart, J. F. *ChemPhysChem* **2005**, *6*, 2145–2152.

(11) (a) Shibasaki, M.; Stoddart, J. F. Vögtle, F. In *Stimulating Concepts in Chemistry*; Wiley-VCH: Weinheim, 2000; pp 211−220. (b) Ashton, P. R.; Baxter, I.; Fyfe, M. C. T.; Raymo, F. M.; Spencer, N.; Stoddart, J. F.; White, A. J. P.; Williams, D. J. *J. Am. Chem. Soc.* **1998**, *120*, 2297–2307. (c) Chiu, S.-H.; Rowan, S. J.; Cantrill, S. J.; Glink, P. T.; Garrell, R. L.; Stoddart, J. F. *Org. Lett.* **2000**, *2*, 3631–3634. (d) Jeppesen, J. O.; Becher, J.; Stoddart, J. F. *Org. Lett.* **2002**, *4*, 557–560. (e) Sohgawa, Y.; Fujimori, H.; Shoji, J.; Furusho, Y.; Kihara, N.; Takata, T. *Chem. Lett.* **2001**, 774–775.

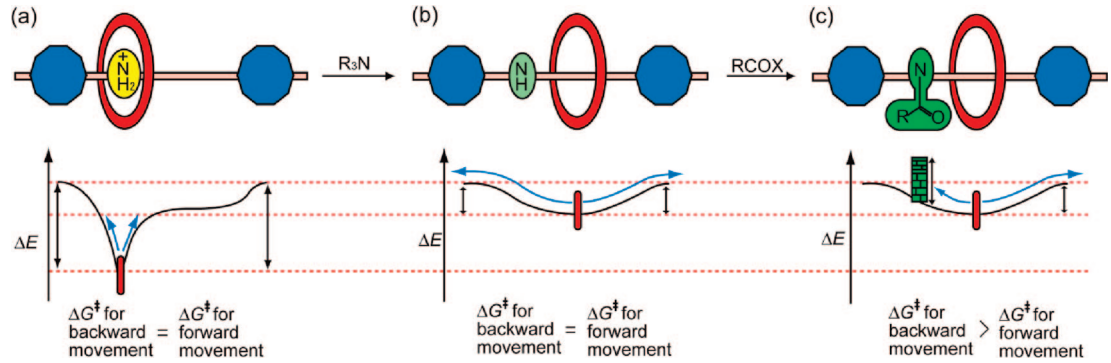

FIGURE 2. Concept of unidirectional transposition of the wheel component in rotaxane. (a) The crown ether wheel is trapped at the ammonium station. (b) By neutralization of the ammonium group, the wheel component is released from the station. Due to the bulky end-cap, the wheel tentatively migrates to the center of the axle. (c) Before the thermal nonselective dethreading of the axle component, a bulky acyl group is introduced on the amino group to prevent dethreading beyond nitrogen.

SCHEME 1

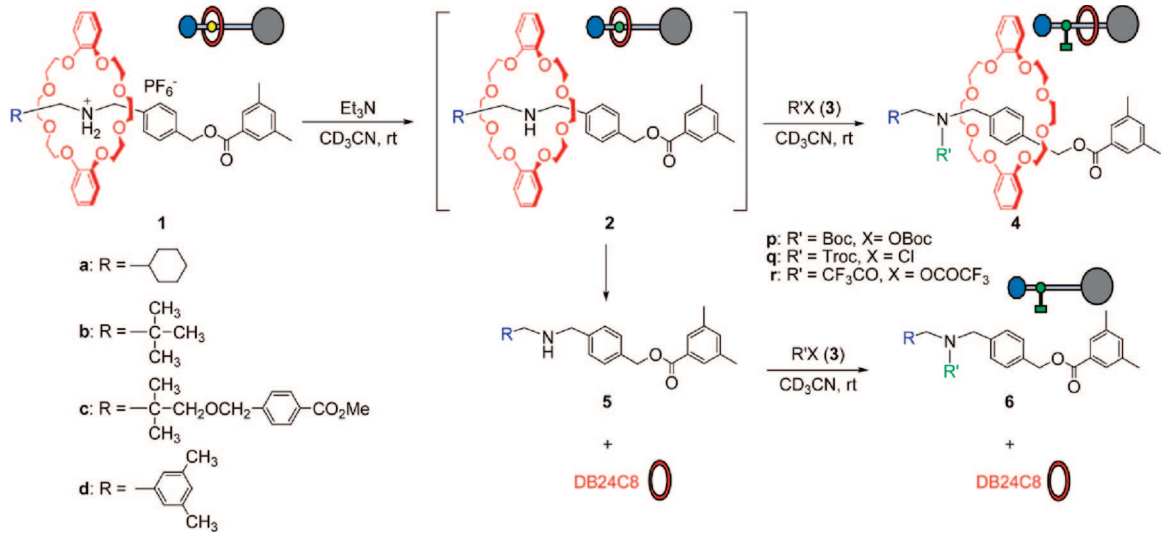

First, the cyclohexyl group was used as the proximate end-cap (rotaxane **1a**) because it is known to be slightly smaller than the cavity of DB24C8.[11] Although **1a** was stable even at 353 K in CD_3CN, deprotonative degradation started when it was treated with 10 equiv of triethylamine at 333 K, thereby forming **5a** and DB24C8 ($\tau_{1/2}$ = 1.3 h). Since deprotonated rotaxane **2a** could not be detected in the ^{1}H NMR spectrum, it can be concluded that deprotonation process is slow. We have observed that deprotonation of ammonium-type rotaxane that has only one station on the axle is very slow.[10] Therefore, the distribution of the wheel component on the axle is expected to be fixed if the acylation is rapid.

To drive the linear molecular motor by acylation, the secondary ammonium group must be reproduced after one-step transposition. Therefore, deprotectable acylation reagents were used for the acylation experiments. If more than one independent deprotection mode can be used, the linear molecular motor can be designed easily. Thus, Boc_2O (**3p**), 2,2,2-trichloroethoxycarbonyl chloride (TrocCl) (**3q**), and TFAA (**3r**) were used as the acylation reagents because corresponding amide can be quantitatively deprotected by acid, reduction, and base, respectively.

TABLE 1. Result of *N*-Acylation and Dethreading of Rotaxane[a]

			yield (%)[b]		
1	**3**	DMAP (equiv)	**4**	**6**	efficiency of active transport[c] (%)
1a	**3p**	0[d]	28	37	43
1a	**3p**	0.1	56	37	60
1a	**3p**	1.0	79	21	79
1b	**3p**	1.0	99	1	99
1c	**3p**	1.0	97 (88)	3	97
1c	**3q**	1.0	98 (92)	2	98
1c	**3r**	0	100 (95)	ND[e]	99

[a] Initial concentration: [**1**] = 15 mM. The reactions were carried out at room temperature for 15 min in CD_3CN in the presence of 5.0 equiv of Et_3N. [b] Determined by the ^{1}H NMR spectra of the crude product (isolated yield given in parentheses). [c] [**4**]/[**4**] + [**6**] [d] The reaction was carried out for 24 h. [e] Not detected.

When **1a** was treated with **3p**[12] in CD_3CN in the presence of 10 equiv of Et_3N, rotaxane **4ap**, in which the wheel component migrated to the distant end-cap, was obtained in 28% yield, while the dethreading product **6ap** was obtained in 37% yield (Table 1). Since acylation of free amine is rapid, neither **2** nor **5** was observed in the crude product. Since **4ap** is thermodynamically less stable than **6ap**, the efficiency of active transport was calculated to be 43%. To accelerate the acylation, 4-dimethylaminopyridine (DMAP) was added to the system as a catalyst. The yield of **4ap** increased with the amount of DMAP as expected. Therefore, the rapid acylation enhanced the

(12) (a) Cao, J.; Fyfe, M. C. T.; Stoddart, J. F. *J. Org. Chem.* **2000**, *65*, 1937–1946. (b) Chiu, S.−H.; Elizarov, A. M.; Glink, P. T.; Stoddart, J. F *Org. Lett.* **2002**, *4*, 3561–3564.

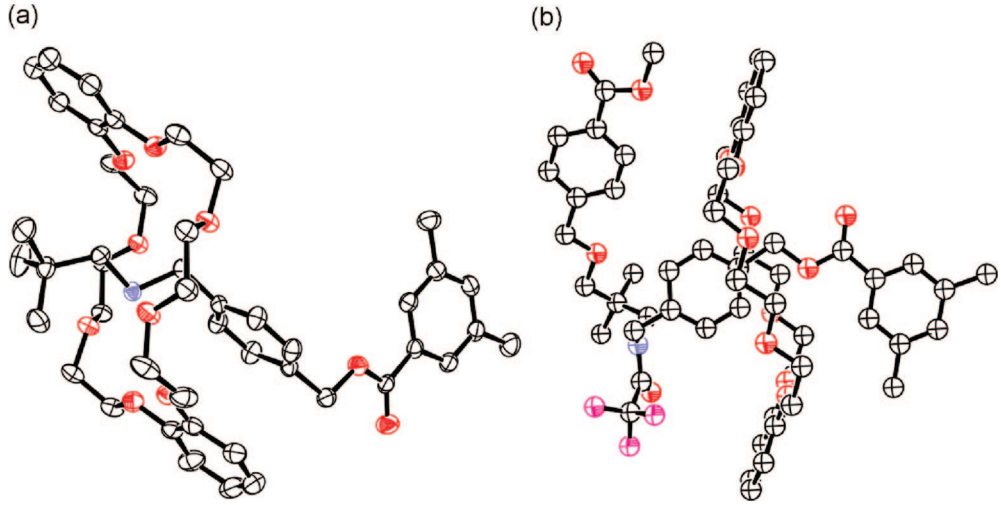

FIGURE 3. Crystal structure of **1b** and **4cr** obtained by X-ray crystallographic analysis. (a) ORTEP drawing of **1b**. Hydrogens and PF_6^- were omitted for clarity. (b) ORTEP drawing of **4cr**. Hydrogens were omitted for clarity.

SCHEME 2

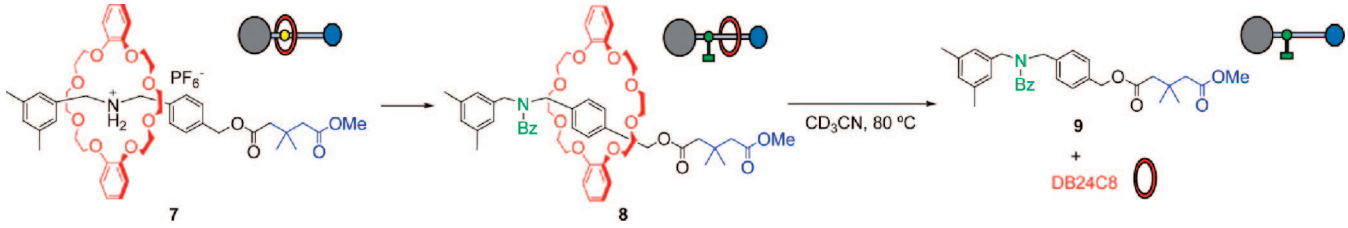

efficiency of active transport. However, **6ap** was still obtained even when 1 equiv of DMAP was used.

To produce a steeper potential surface, a more bulky *tert*-butyl group was employed as the proximate end-cap (rotaxane **1b**).[13] The structure of **1b**, as determined by X-ray crystallographic analysis, is shown in Figure 3a. Owing to the bulkiness of the *tert*-butyl group, the deprotonative degradation of **1b** was very slow ($\tau_{1/2}$ = 198 h at 333 K) in the presence of 10 equiv of triethylamine. **1b** was then treated with **3p** in the presence of triethylamine, and **4bp** was obtained in 99% yield along with only 1% of **6bp**. As expected, the slow dethreading due to a steeper potential surface in **2b** drastically prevented the formation of **6bp** to improve the efficiency of the active transport.

Encouraged by this result, a neopentyl-type end-cap group that is suitable for the construction of a polymeric track with a periodic potential was employed as the proximate end-cap (rotaxane **1c**). As expected, the neopentyl-type end-cap in **1c** and the *tert*-butyl group in **1b** behaved similarly, and a good yield of the desired rotaxane **4cp** was obtained in the reaction with **3p**. For faster acylation, other acylation reagents were examined. The selectivity of **4c** increased slightly with 2,2,2-trichloroethoxycarbonyl chloride (TrocCl) (**3q**), and the quantitative formation of **4cr** was achieved when TFAA (**3r**) was used as the acylation reagent. Owing to the high reactivity of **3r**, the addition of DMAP was not necessary. The structure of **4cr** was confirmed by X-ray crystallographic analysis, as shown in Figure 3b.

The simple first order kinetics ($\tau_{1/2}$ = 462 h at 333 K in CD_3CN) was followed by the deprotonative decomposition of **1c** that was caused by treating it with 10 equiv of triethylamine to produce **5c**. Therefore, it was confirmed that the dethreading of **1c** to form **5c** is a thermodynamically favored process in the presence of triethylamine. Since **1d**[10] is stable under the same condition, it is evident that the wheel component in **2c** dethreaded the axle component beyond the neopentyl-type end-cap, but not beyond the 3,5-dimethylphenyl end-cap. Therefore, the migration of the wheel component toward the proximate end-cap is thermodynamically favored movement for **1c** during the treatment with triethylamine. However, in the acylation experiments, the wheel in **1c** migrated toward the distant end-cap—a thermodynamically undesired direction—to produce **4cr** quantitatively. Therefore, the movement is the active transport, which was achieved by the local potential surface on the axle of **1c** and **2c**.The effect of the neopentyl-type group as the distant end-cap was examined. Thus, rotaxane **7** having neopentyl-type distant end-cap was prepared (Scheme 2).[13] Rotaxane **7** was stable even at 333 K in DMSO that strongly inhibits the hydrogen bonding interaction. Due to the hydrogen bonding interaction that was working between wheel and axle even in DMSO, the neopentyl group acted as the effective end-cap.[14] Acylative neutralization of **7** by benzoyl chloride afforded the corresponding rotaxane **8**.

Dethreading of **8** occurred rapidly at 333 K in CD_3CN to form **9** and DB24C8 ($\tau_{1/2}$ = 1.2 h) in the absence of triethylamine. These results indicate the diversed effect of the neopentyl-type group as the distant end-cap. When the interaction between the axle and the wheel is working, the neopentyl group acts as the sufficiently bulky end-cap to produce the steep potential. However, without the intercomponent interaction, the neopentyl-type group behaves as the sufficiently small end-cap to allow the dethreading of the wheel component.

(13) Makita, Y.; Kihara, N.; Takata, T. *Chem. Lett.* **2007**, 102–103.

(14) Tachibana, Y.; Kihara, N.; Furusho, Y.; Takata, T. *Org. Lett.* **2004**, *6*, 4507–4509.

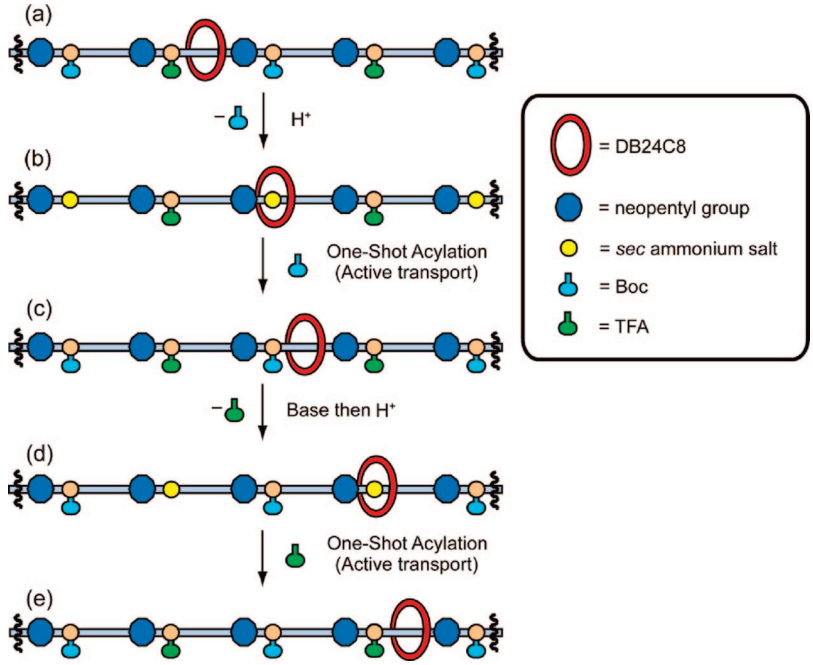

FIGURE 4. Schematic representation of the unidirectional migration of the wheel component on a polymeric track. (a) The linear molecular motor consists of [2]rotaxane in which the axle is made of polyammonium salt, and every ammonium salt moiety is separated by a neopentyl group. The ammonium salt moieties on the axle track are alternatively acylated by the Boc group (light blue) and the TFA group (green). (b) The Boc group is deprotected in order to reproduce the ammonium salt moiety. The wheel component migrates to the thermodynamically stable ammonium salt station. (c) The ammonium groups are acylated by Boc (one-shot acylation). The wheel component unidirectionally migrates to the space between the Boc and the neopentyl groups. (d) The selective deprotection of the TFA group is followed by application of protonation forces to the wheel component in order to move it to the thermodynamically stable ammonium salt station. (e) The ammonium group is acylated by TFAA (one-shot acylation). The wheel component unidirectionally migrates to the space between the TFA and the neopentyl groups.

Conclusions

We have investigated the quantitative active transport of the wheel component of rotaxane. The transport of the wheel is controlled by a neopentyl end-cap. The direction of transport is influenced by the local potential surface and not by the thermodynamic stability. In other words, it is driven by the gradient of the local potential surface and the free energy due to acylation and not as a result of attractive interactions. These features are an essential part of chemical energy-driven unidirectional linear molecular motors. Thus, an artificial linear molecular motor system can be envisioned to be a simple extension of the transport system illustrated in Figure 4.

The designed unidirectional linear motor consists of [2]rotaxane with a polymeric ammonium salt axle. The ammonium salt moieties are separated by neopentyl groups and are alternatively protected by two types of independent deprotectable acyl groups such as Boc and TFA. This system is referred by the alternating copolymer of **4 cp** and **4cr**. When a Boc group (light blue protection) is selectively deprotected by acid, the wheel component moves in a unidirectional manner to the next ammonium moiety beyond the neopentyl group. The resulting ammonium rotaxane is also protected by Boc. We have demonstrated that the wheel component can undergo quantitative active transport because of the steep potential surface created by the neopentyl group. The next step is the selective deprotection of TFA by alkaline hydrolysis, which is followed by protonation in order to force the wheel to migrate to the next ammonium group in a unidirectional manner. We can expect that the treatment of the resulting rotaxane by TFAA results in the recovery of the first condition of the linear molecular motor although the wheel component unidirectionally forwarded two steps.

The active transport of the wheel was driven by a one-shot acylation reaction that corresponded to the phosphorylation by ATP. Therefore, the present work demonstrates that the features of natural molecular motors can be realized in simple molecular systems by a simple reaction that utilizes the local potential surface. We are currently focusing our efforts toward the synthesis of poly[2]rotaxane, which behaves as a linear molecular motor.

Experimental Section

Rotaxane (1a): ^{1}H NMR (500 MHz,$CDCl_3$) 7.67 (s, 2H), 7.55 (d, J = 8.3 Hz, 2H), 7.36 (d, J = 8.3 Hz, 2H), 7.21 (s, 1H), 7.05 (brs, 2H), 6.92−6.85 (m, 8H), 5.31 (s, 2H), 4.70−4.67 (m, 2H), 4.25−4.22 (m, 4H), 4.12−4.09 (m, 4H), 3.84−3.76(m, 8H), 3.60−3.56 (m, 4H), 3.33−3.30 (m, 4H), 2.89−2.86 (m, 2H), 2.37 (s, 6H), 1.54−1.23 (m, 6H), 0.94−0.90 (m, 3H), 0.60−0.57 (m, 2H); ^{13}C NMR (125 MHz, $CDCl_3$) δ 166.7, 147.7, 138.3, 137.8, 135.0, 132.4, 130.5, 123.0, 128.1, 127.5, 122.0, 113.1, 70.9, 70.3, 68.6, 65.9, 55.6, 52.6, 35.9, 30.4, 25.8, 25.5, 21.3; mp 69−70 °C; HRMS (ESI-TOF) calcd for $C_{48}H_{64}N_1O_{10}$ 814.4530 ([M − PF_6]$^+$), found814.4523 [M − PF_6]$^+$. Anal. Calcd for $C_{48}H_{64}F_6NO_{10}P$: C, 60.05; H, 6.72; N, 1.46. Found: C, 59.69; H, 6.47; N, 1.25.

Rotaxane (1b): ^{1}H NMR (500 MHz,$CDCl_3$) δ 7.69−7.67 (m, 4H), 7.37 (d, J = 8.3 Hz, 2H), 7.21 (s, 1H), 6.94−6.87 (m, 10H), 5.33 (s, 2H), 4.72−4.70 (m, 2H), 4.29−4.25 (m, 4H), 4.15−4.11 (m, 4H), 3.81−3.75 (m, 8H), 3.60−3.57 (m, 4H), 3.30−3.27 (m, 4H), 3.03−3.00 (m, 2H), 2.36 (s, 6H), 0.76 (s, 6H); ^{13}C NMR (125 MHz, $CDCl_3$) δ 166.7, 147.8, 138.3, 138.1, 131.7, 131.3, 130.0, 128.0, 127.5, 122.0, 113.1, 71.1, 70.5, 68.6, 65.9, 61.5, 53.7, 30.4, 27.1, 21.3; mp 188−189 °C; HRMS (ESI-TOF) calcd for $C_{46}H_{62}N_1O_{10}$ 788.4368 ([M − PF_6]$^+$), found 788.4366 [M − PF_6]$^+$.

Rotaxane (1c): ^{1}H NMR (500 MHz, $CDCl_3$) δ 7.95 (d, 2H, 8.3 Hz), 7.66 (s, 2H), 7.61 (d, 2H, 8.3 Hz), 7.36−7.20 (m, 5H), 6.93−6.84 (m, 10H), 5.29 (s, 2H) 4.75−4.72 (m, 2H), 4.29 (s, 2H),

4.22−4.20 (m, 4H), 4.11−4.08 (m, 4H), 3.91 (s, 3H), 3.77−3.72 (m, 8H), 3.59−3.56 (m, 4H), 3.33−3.27 (m, 6H), 2.97 (s, 2H), 2.35 (s, 6H), 0.86 (s, 6H); ^{13}C NMR (125 MHz, $CDCl_3$) δ 167.0, 166.7, 147.7, 143.5, 138.3, 137.9, 135.0, 131.7, 131.1, 129.9, 129.7, 129.5, 128.4, 127.9, 127.4, 127.3, 121.9, 112.9, 77.6, 72.6, 71.0, 70.4, 68.4, 65.9, 58.0, 53.8, 52.2, 34.7, 22.1, 21.3; mp 149−150 °C; HRMS (FAB-MS) calcd for $C_{55}H_{70}NO_{13}$ 952.4842 ([M − PF_6]$^+$), found 952.4856 [M − PF_6]$^+$. Anal. Calcd for $C_{55}H_{70}F_6NO_{13}P$: C, 60.16; H, 6.43; N, 1.28. Found: C, 59.96; H, 6.23; N, 1.26.

General Procedure for the Neutralization-Induced Dethreading of Rotaxane. A solution of rotaxane (5.4 μmol) and triethylamine (7.0 μL, 54 μmol) in CD_3CN (0.60 mL) was allowed to stand at 60 °C. The progress of the dethreading was monitored by ^{1}H NMR.

General Procedure for N-Acylation. A solution of rotaxane (5.4 μmol), acylation reagent (0.54 mmol), triethylamine (7.0 μL, 54 μmol), and DMAP (0.7 mg, 0.54 μmol) in CD_3CN (0.60 mL) was allowed to stand at room temperature for 0.5 h. After water was added, the mixture was extracted by chloroform. The organic layer was dried over magnesium sulfate and evaporated in vacuo. The crude product was purified by preparative gel permeation chromatography (chloroform) to afford *N*-acylated rotaxane and the dethreading product.

N-Acylated rotaxane (4bp): ^{1}H NMR (500 MHz, $CDCl_3$) δ 8.16−8.11 (m, 4H), 7.09 (s, 1H), 7.00−6.94 (m, 2H), 6.89−6.81 (m, 8H), 5.98 (two s, 2H), 4.66, 4.37 (two s, 2H), 4.10−4.03 (m, 8H), 3.73−3.71 (m, 4H), 3.64−3.62 (m, 4H), 3.27−3.23 (m, 4H), 2.96−2.85 (m, 6H), 2.21 (s, 6H), 1.51, 1.49 (two s, 9H), 0.92, 0.89 (two s, 9H); ^{13}C NMR (125 MHz, $CDCl_3$) δ 167.2, 148.6, 137.8, 134.2, 129.4, 129.3, 128.4, 127.3, 126.6, 125.1, 120.6, 111.6, 84.5, 69.7, 69.5, 69.4, 68.0, 66.9, 57.4, 53.4, 52.7, 34.3, 33.8, 28.5, 28.4, 27.7, 21.0; mp 96−98 °C; ESI-MS *m*/*z* 910.10 [M + Na]$^+$. Anal. Calcd for $C_{51}H_{69}NO_{12}$: C, 68.97; H, 7.83; N, 1.58. Found: C, 68.68; H, 7.58; N, 1.45.

N-Acylated rotaxane (4cp): ^{1}H NMR (500 MHz, $CDCl_3$) δ 8.15, 8.14 (two s, 2H), 8.10 (brs s, 2H), 8.00−7.98 (m, 2H), 7.35−7.33 (m, 2H), 7.07 (m, 2H), 7.03−6.94 (m, 2H), 6.86−6.79 (m, 8H), 4.54, 4.44 (two s, 2H), 4.42, 4.33 (two s, 2H), 4.08−4.01 (m, 8H), 3.90, 3.89 (two s, 2H), 3.72−3.60 (m, 8H), 3.27−3.23 (m, 4H), 3.17, 3.04 (two s, 2H), 3.13, 3.11 (two s, 2H), 2.90−2.86 (m, 4H), 2.20 (s, 6H), 1.48, 1.48 (two s, 9H), 0.95, 0.91 (two s, 9H); ^{13}C NMR (125 MHz, $CDCl_3$) δ 167.2, 167.1, 148.6, 137.7, 134.2, 134.0, 131.0, 129.8, 129.5, 129.4, 128.4, 127.2, 127.2, 127.1, 126.4, 120.6, 111.6, 84.6, 72.7, 72.6, 69.7, 69.5, 69.4, 68.0, 66.9, 53.8, 53.1, 53.0, 52.4, 52.2, 38.1, 37.7, 29.9, 27.7, 23.8, 23.7, 21.0; mp 58−59 °C; HRMS (FAB-MS) calcd for $C_{60}H_{77}NNaO_{15}$ 1074.5185 ([M + Na]$^+$), found 1074.5145 ([M + Na]$^+$).

N-Acylated rotaxane (4cq): ^{1}H NMR (500 MHz, $CDCl_3$) δ 8.19−8.16 (m, 2H), 8.11−8.08 (m, 2H), 8.00−7.98 (m, 2H), 7.38−7.33 (m, 2H), 7.09−7.07 (m, 1H), 7.03−6.98 (m, 2H), 6.89−6.80 (m, 8H), 5.97, 5.96 (two s, 2H), 4.69, 4.54 (two s, 2H), 4.50−4.40 (m, 4H), 4.10−4.01 (m, 8H), 3.90, 3.88 (two s, 3H), 3.70−3.60 (m, 8H), 3.23−3.12 (m, 8H), 2.85−2.80 (m, 4H), 2.20, 2.19 (two s, 6H), 0.93−0.94 (m, 6H); ^{13}C NMR (125 MHz, $CDCl_3$) δ 167.1, 148.6, 137.9, 131.0, 129.8, 129.2, 129.0, 128.3, 127.1, 126.5, 120.6, 111.6, 72.7, 69.7, 69.4, 69.3, 68.0, 66.8, 52.2, 38.1, 24.0, 23.8, 20.9; mp 48−50 °C; HRMS (FAB-MS) calcd for $C_{58}H_{70}Cl_3NO_{15}$ 1125.3811 ([M]$^+$), found 1125.3822 ([M]$^+$). Anal. Calcd for $C_{58}H_{70}Cl_3NO_{15}$: C, 61.78; H, 6.26; N, 1.24. Found: C, 61.42; H, 6.06; N, 1.42.

N-Acylated rotaxane (4cr): ^{1}H NMR (500 MHz, $CDCl_3$) δ 8.20 (d, 2H, J = 8.3 Hz), 8.11 (s, 2H), 7.98 (d, 2H, J = 8.3 Hz), 7.33 (d, 2H, J = 8.3 Hz), 7.10 (s, 1H), 6.88−6.81 (m, 8H), 5.97 (s, 2H), 4.52 (s, 2H), 4.51 (s, 1H), 4.09−4.01 (m, 4H), 3.89 (s, 3H), 3.71−3.68 (m, 4H), 3.61−3.58 (m, 4H), 3.42−3.21 (m, 4H), 3.17 (s, 2H), 3.16 (s, 2H), 2.84−2.81 (m, 4H), 2.22 (s, 6H), 0.94 (s, 6H); ^{13}C NMR (125 MHz, $CDCl_3$) δ 168.7, 168.6, 167.4, 148.6, 148.6, 145.6, 138.7, 138.3, 137.9, 137.7, 134.4, 130.9, 129.5, 129.5, 129.3, 129.2, 129.1, 128.6, 128.5, 126.5, 126.1, 125.6, 124.2, 120,7, 120.5, 113.0, 111.6, 111.4, 106.4, 69.8, 69.6, 69.4, 68.1, 67.6, 50.9, 47.8, 29.9, 24.5, 21.7, 21.5, 21.4, 21.0; mp 126−127 °C; HRMS (FAB-MS) calcd for $C_{57}H_{68}F_3NO_{14}$ 1047.4592 ([M]$^+$), found 1047.4606 ([M]$^+$).

Rotaxane (7)[13]: ^{1}H NMR (500 MHz, $CDCl_3$) δ 7.56 (brs, 2H), 7.35 (d, 2H, J = 8.3 Hz), 7.20 (d, 2H, J = 8.3 Hz), 6.91−6.88 (m, 4H), 6.84 (s, 1H), 6.81−6.79 (m, 4H), 5.01 (s, 2H), 4.66−4.63 (m, 2H), 4.46−4.44 (m, 2H), 4.11−4.10 (m, 8H), 3.78−3.77 (m, 8H), 3.63 (s, 3H), 3.50−3.43 (m, 8H), 2.49 (s, 2H), 2.42 (s, 2H), 1.10 (s, 6H); ^{13}C NMR (125 MHz, $CDCl_3$) δ 172.4, 171.7, 147.6, 138.5, 137.5, 131.7, 131.5, 130.8, 129.7, 128.2, 126.8, 121.8, 112.8, 70.8, 70.3, 68.3, 65.3, 52.8, 52.4, 51.4, 45.1, 32.8, 27.7, 21.3; mp 48−49 °C; HRMS (ESI-TOF) calcd for $C_{49}H_{66}NO_{12}$ 860.4580 ([M − PF_6]$^+$), found 860.4561 [M − PF_6]$^+$. Anal. Calcd for $C_{49}H_{66}F_6NO_{12}P$: C, 58.50; H, 6.61; N, 1.39. Found: C, 58.50; H, 6.94; N, 1.55.

N-Acylated rotaxane (8): ^{1}H NMR (500 MHz, CD_3CN, 333K) δ 7.87 (d, 2H, J = 7.8 Hz), 7.41−7.37 (m, 6H), 6.93−6.87 (m, 10H,), 6.76 (brs, 2H), 5.66 (s, 2H), 4.38 (brs, 4H), 4.13−4.03 (m, 8H), 3.69−3.63 (m, 8H), 3.53 (s, 3H), 3.39−3.34 (m, 4H), 3.07 (brs, 4H), 2.41 (s, 2H), 2.30 (s, 2H), 2.25 (s, 6H), 0.89 (brs, 6H).

Decomposition of Rotaxane (8).[14] A solution of rotaxane **8** (5.4 μmol) in CD_3CN (0.60 mL) was allowed to stand at 333 K. The progress of the dethreading was monitored by ^{1}H NMR.

Acknowledgment. This work was funded by the Sasakawa Scientific Research Grant from The Japan Science Society.

Supporting Information Available: Experimental details, spectroscopic and analytical data for new compounds, and X-ray crystallographic files (CIF) for rotaxane **1b** and **4cr**. This material is available free of charge via the Internet at http://pubs.acs.org.

JO8013726